

Contents lists available at ScienceDirect

Chemosphere

journal homepage: www.elsevier.com/locate/chemosphere



Low dose lead exposure induces alterations on heterochromatin hallmarks persisting through SH-SY5Y cell differentiation



Li F. Lin ^{a, 1}, Junkai Xie ^a, Oscar F. Sánchez ^b, Chris Bryan ^c, Jennifer L. Freeman ^{d, e}, Chongli Yuan ^{a, e, *}

- ^a Davidson School of Chemical Engineering, Purdue University, West Lafayette, IN, 47907, USA
- ^b Department of Nutrition and Biochemistry, Pontificia Universidad Javeriana, Bogotá, 110231, Colombia
- ^c Department of Statistics, Purdue University, West Lafayette, IN, 47907, USA
- ^d School of Health Sciences, Purdue University, West Lafayette, IN, 47907, USA
- ^e Purdue University Center for Cancer Research, West Lafayette, IN, 47907, USA

HIGHLIGHTS

- Exposure to Pb prior to differentiation alters the morphology of neurons.
- Alterations in 5 mC persist and attenuate after removal of exposure.
- Differentiation amplifies changes in 5 mC acquired from Pb exposure.
- Changes in 5 mC shows a strong correlation with phenotypical alterations.
- Pb-induced changes in H3K9me3 & H3K27me3 are (over)compensated for after Pb removal.

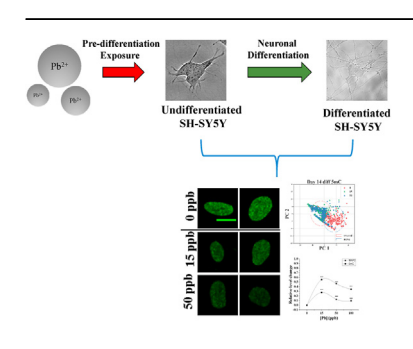
ARTICLE INFO

Article history:
Received 29 July 2020
Received in revised form
28 September 2020
Accepted 28 September 2020
Available online 1 October 2020

Handling Editor: A. Gies

Keywords: Lead exposure 5 mC H3K9me3 H3K27me3 Epigenetic persistence

G R A P H I C A L A B S T R A C T



ABSTRACT

Lead (Pb) is a commonly found heavy metal due to its historical applications. Recent studies have associated early-life Pb exposure with the onset of various neurodegenerative disease. The molecular mechanisms of Pb conferring long-term neurotoxicity, however, is yet to be elucidated. In this study, we explored the persistency of alteration in epigenetic marks that arise from exposure to low dose of Pb using a combination of image-based and gene expression analysis. Using SH-SY5Y as a model cell line, we observed significant alterations in global 5-methycytosine (5 mC) and histone 3 lysine 27 tri-methylation (H3K27me3) and histone 3 lysine 9 tri-methylation (H3K9me3) levels in a dose-dependent manner immediately after Pb exposure. The changes are partially associated with alterations in epigenetic enzyme expression levels. Long term culturing (14 days) after cease of exposure revealed persistent changes in 5 mC, partial recovery in H3K9me3 and overcompensation in H3K27me3 levels. The observed alterations in H3K9me3 and H3K27me3 are reversed after neuronal differentiation, while reduction in 5 mC levels are amplified with significant changes in patterns as identified via texture clustering analysis. Moreover, correlation analysis demonstrates a strong positive correlation between trends of 5 mC alteration after differentiation and neuronal morphology. Collectively, our results suggest that exposure to low dose of Pb prior to differentiation can result in persistent epigenome alterations that can potentially be responsible for the observed phenotypic changes. Our work reveals that Pb induced

^{*} Corresponding author. Davidson School of Chemical Engineering, Purdue University, West Lafayette, IN 47907, USA. *E-mail address:* cyuan@purdue.edu (C. Yuan).

¹ Current address: Department of Chemical and Biomolecular Engineering, University of California, Berkeley, CA 94704,USA.

changes in epigenetic repressive marks can persist through neuron differentiation, which provides a plausible mechanism underlying long-term neurotoxicity associated with developmental Pb-exposure.

© 2020 Elsevier Ltd. All rights reserved.

1. Introduction

Lead (Pb) is a heavy metal historically used for various applications, i.e., painting, ceramic glazing, pipe soldering, and gasolines (Nriagu, 1990; Wilson and Horrocks, 2008) and is thus found in soil and water sources due to its historical uses (Annest et al., 1983; Obeng-Gyasi, 2019). A survey conducted in late 1970s suggested that ~78% of the population has blood lead levels (BLLs) of 10 µg/dL (100 parts per billion, ppb) or higher; and this percentage is even higher in children (1–5 years old) with an estimated percentage of 88% (Dignam et al., 2019). Usage of Pb has thus been tightly regulated by environmental protection agencies. High Pb levels exceeding the regulatory standard, however, are often reported in many geographic locations due to legacy uses. Human exposure to Pb can primarily be attributed to ingestion of contaminated food (~59–81% of total Pb exposure cases (Watanabe et al., 2000)) or water (~20% of total (Jarvis et al., 2018)).

Pb exposure can happen at different life stages. Among them, developmental exposure to Pb is often associated with more detrimental health outcomes, including severe damages in central nervous system (Nevin, 2000, 2007) and thus has attracted significant attention in recent years. Specifically, children with prenatal Pb exposure at a maternal blood level of 1.52 μ g/L (ppb) during late pregnancy (near delivery with a median of 39-week), have lower mental development index (Kim et al., 2013), while children exposed to Pb at young ages show severe impairment in their cognitive functions and often poor academic performances (Cecil et al., 2008). Interestingly, post-natal exposure to low concentrations of Pb (<7.5 μg/L, ppb) seems to cause more significant damages than prenatal exposure (Bellinger et al., 1992'bib_Bellinger_et_al_1987'bib_Bellinger_et_al_1992; Lanphear et al., 2000). Pathologically, exposure to Pb during childhood (<6.5 years old) can cause significant changes in brains at adulthood (19-24 years old) including alterations in brain volume, architecture and metabolism (Cecil et al., 2011). Recent studies have further associated early-life Pb exposure to various neurodegenerative disorders, such as Alzheimer's disease (AD) (Eid et al., 2016; Bihaqi et al., 2017) and Parkinson's disease (PD) (Weisskopf et al., 2010; Caudle et al., 2012) aligning with the Developmental Origins of Health and Disease (DOHaD) paradigm. Collectively, these results have led to the recent revision of action doses of Pb in drinking water from 50 to 15 ppb by the U.S. Environmental Protection Agency.

The neurotoxicity of Pb, in the form of Pb²⁺, partially arises from its resemblance to other cations essential for neuron activities, such as Ca (Ca²⁺) and Na (Na⁺) (Needleman, 2004). Specifically, Pb competes with Ca in neuronal signaling pathways (Flora et al., 2012; Meissner, 2017) and can disrupt the excitatory and inhibitory synaptic transmission balance in hippocampal neurons (Zou et al., 2020). Pb can also interfere with Na uptake and subsequently affect neuron firing (Yan et al., 2008). The long-term health implications of Pb exposure, particularly increased risk for AD and PD (Coon et al., 2006; Mansouri and Cauli, 2009; Weisskopf et al., 2010; Caudle et al., 2012; Eid et al., 2016; Bihaqi et al., 2017), however, cannot be fully explained by such a mechanism. This knowledge gap hinders the development of effective intervention approaches to reverse long-term neurotoxicity induced by Pb-

exposure. Nevertheless, a recent zebrafish study (Meyer et al., 2020) shown Pb exposure has transgenerational effects in altering brain transcriptome, suggesting the involvement of epigenetic mechanism accounting for low mutagenic activities of Pb at low doses.

Recent studies have been associating exposure to Pb with epigenome changes. For example, developmental Pb exposure in mice can cause expression changes in DNA methyltransferase 1 (DNMT1), DNA CpG methylation (^{me}CpG) and other histone modification levels, including H3K9ac, H3K4me2 and H3K27me3 (Eid et al., 2016). Similar observations were also made in rats (Singh et al., 2018a). Pb can also affect the activities of epigenetic enzymes, i.e., DNMTs as shown in our previous study (Sanchez et al., 2017). However, these studies focused on acute responses from Pb exposure and did not assess the persistence of Pb-induced epigenetic changes after removal of Pb treatment. It thus remains elusive as to how epigenetic changes induced by Pb exposure can persist through the developmental stage and confer long-term health risks after the cessation of exposure to Pb.

Here, we worked with SH-SY5Y cell line, a model human neuroblastoma cell line capable of differentiating into neurons (Xicoy et al., 2017) to examine epigenetic changes induced by exposure to Pb that potentially persist after the cessation of exposure. Exposure to low doses of Pb (15 and 50 ppb) prior to differentiation is found to induce significant changes in the percentage of mature neurons as well as neurite lengths. Significant epigenetic changes were observed right after Pb exposure potentially attributing to expression changes in epigenetic enzyme. Changes in 5 mC levels persist after cessation of exposure and amplifies through neuronal differentiation, suggesting a potential correlation with the observed nonlinear dose-dependence of phenotypical alteration. Our findings here, collectively, offer a novel perspective and progress towards the elucidation of mechanisms underlying Pb associated long-term neurotoxicity.

2. Material and methods

2.1. Culture and differentiation of SH-SY5Y

SH-SY5Y (ATCC, CRL-2266) was cultured following the standard protocol recommended by the manufacturer. Specifically, cells were maintained in Eagle's Minimum Essential Medium (Gibco, U.S.) supplemented with 10% (v/v) fetal bovine serum (Atlanta Bio, U.S.), 1% of Penicillin-Streptomycin and 1% of MEM Non-Essential Amino Acids (Gibco, U.S.). Cells were passed in T25 flasks at 37 °C with 5% $\rm CO_2$.

SH-SY5Y differentiation was carried out following a protocol adapted from literature (Shipley et al., 2016) (see also Fig. 1A). Briefly, differentiation was started on Day 0 by an exchange of culture medium, proceeded to Day 6 with a second medium exchange and completed on Day 14. Compositions of differentiation medium can be found in Table S1 (Supplementary information). The completion of differentiation was confirmed by staining cells with MAP2-antibody (PA5-17646, Invitrogen, U.S.) that are specific for mature neurons.

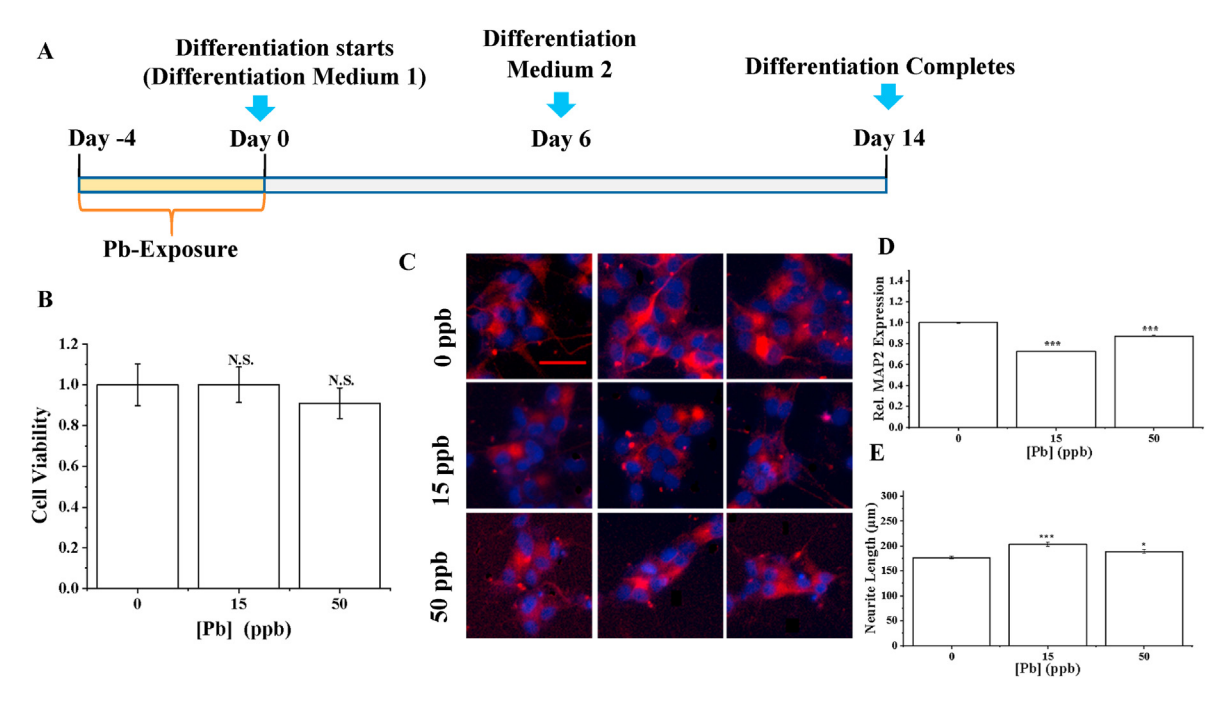


Fig. 1. (A) A schematic illustration of the exposure and differentiation timeline for SH-SY5Y cells. (**B**) Viability of cells after exposure to Pb of different doses for 96 h assayed using MTT. Data = mean \pm standard deviation. n = 3. (**C**) Differentiated SH-SY5Y cells (Day 14) were stained with MAP2 antibody (red) and DAPI (blue). Cells were exposed to various concentrations of Pb prior to the initiation of differentiation. Scale bar = 50 μ m (**D**) A bar plot showing relative MAP2 expression levels in Pb-naïve and treated cells. (**E**) Neurite length of differentiated SH-SY5Y neurons that have been exposed to Pb of varying doses. In (**D**) and (**E**), n > 300 cells. N.S.: no significance (p > 0.05). * [=] p < 0.05, *** [=] p < 0.001. Data = mean \pm standard error. (For interpretation of the references to color in this figure legend, the reader is referred to the Web version of this article.)

2.2. Selection of Pb concentrations and treatment

Pb stock solutions were prepared as described previously (Lee et al., 2017) and spiked into cell culture medium at selected concentrations. We have chosen Pb concentrations of 15 and 50 ppb in this work based on the past and current EPA regulation standard on drinking water (50 and 15 ppb, respectively)(2007). Pb concentrations higher than 15 ppb have also been reported in recent public health incidence (e.g., $16.5-33.2 \mu g L^{-1}$ (ppb) (Pieper et al., 2018)).

All cells were treated with Pb of 0, 15 or 50 ppb for 96 h prior to differentiation (see also Fig. 1A) or continuous culturing. All cells were washed three times in PBS prior to the initiation of differentiation or continuous culturing.

2.3. Cell viability and morphological assessments

Cell viability was assessed using a colorimetric MTT assay (ab211091, Abcam, U.S.). Nuclear size and morphology were determined by first staining cell nucleus with Draq5 (Thermo Fisher, U.S.) followed by imaging using fluorescent microscopy (Nikon, Japan). Individual nucleus was identified using a customized CellProfiler (Broad Institute, U.S.) pipeline as we detailed in our previous work (Sánchez et al., 2020).

Neurite length was determined via cell images collected using a bright-field microscope (Floid, Life Technologies) and quantified via the Simple Neurite Tracing plugin in FIJI (NIH, U.S.) (Fanti et al., 2008). Specifically, the length of the longest bifurcation branch of each neuron was measured to characterize the neurite length of each neuron.

2.4. Immunostaining

To characterize the completion of differentiation, all differentiated cells were fixed with 4% paraformaldehyde (Thermo Fisher,

U.S.) followed by permeabilization overnight in 1% Triton-X (Sigma, U.S.). Cells were then stained with anti-MAP2 antibody (1: 200 dilution, PA5-17646, Invitrogen) at 4 °C overnight followed by staining with a secondary goat-anti-rabbit antibody coupled with Alexa 568 (ab175471, Abcam, US).

Immunostaining for selected epigenetic modifications, namely 5 mC, H3K9me3 and H3K27me3, was carried out following a similar protocol as described above. To reduce the bias due to crossreactivity between H3K9me3 and H3K27me3 antibodies, we selected the Abcam antibodies that report low or none crossreactivity (Kungulovski et al., 2014; Keniry et al., 2016) and included a large number of cells (n > 500) in our analysis. An additional denaturation step was included for 5 mC staining, in which the cells are treated with 4 N HCl for 30 min and equilibrated with 100 mM Tris-HCl (pH 8.5) for 10 min 5 mC (61479, Active Motif, U.S.), H3K9me3 (ab8898, Abcam, U.S.) and H3K27me3 (ab192985, Abcam, U.S.) antibodies were used as primary. Goatanti-mouse coupled with Alexa 488 (R37120, Thermo Fisher, U.S.) and Goat-anti-rabbit coupled with Alexa 568 (ab175471, Abcam, US) were used as secondary antibodies for 5 mC and histone modifications, respectively.

2.5. Fluorescent microscopy

All fluorescent images were collected using a Nikon Eclipse Ti-2 inverted microscope. A $60 \times /1.40$ NA oil objective was used for all images. Z-stack of cells were collected using Nikon EZ-C1 software with an interval of 1 μ m. 2D max projections were created with ImageJ as we described previously (Sánchez et al., 2019, 2020). All images were then analyzed using a customized Cell Profiler pipeline similar as we described in our previous publication (Sánchez et al., 2020).

2.6. Gene expression analysis via RT-qPCR

Pellets of SH-SY5Y cells were collected immediately after completion of Pb treatments (96 h) to determine changes in key epigenetic enzymes, namely DNMT1, DNMT3A, DNMT3B and TET1 for 5 mC; KMT1A and KDM4A for H3K9me3, and EZH2, KDM6A and KDM6B for H3K27me3. β-Actin (ACTB) was used as the reference gene. Total RNA was extracted using an RNA purification kit (PureLink, Thermo Fisher Scientific, U.S.) following the manufacturer's protocol and then reverse transcribed using SuperScript IV Reverse Transcriptase (Invitrogen, U.S.) with random hexamer primers. PowerUp SYBR Green (Applied Biosystems, U.S.) was used. Quantitative PCR (qPCR) was performed using QuantStudio 3 (Thermo Fisher, U.S.) following the MIQE guideline (Bustin et al., 2009). All qPCR primers were summarized in Table S2 (Supporting Information).

2.7. Data analysis and statistics

All data were presented as mean \pm standard deviation unless otherwise specified with independent replicates \geq 3. All statistical analysis and calculations were performed using OriginPro (Version, 2019; North Hampton, MA) statistical software. Analysis of variance and Tukey's post-hoc test was used to calculate significance at different p-values. Principle Component Analysis and k-means clustering analysis was performed using Jupyter Notebook.

3. Results

3.1. Exposure to low dose of Pb affects SH-SY5Y differentiation

SH-SY5Y cells were treated with 0, 15 or 50 ppb of Pb prior to differentiation for 96 h (4 days) following the scheme outlined in Fig. 1A. The dose of Pb was selected based on the current regulation standard while accounting for Pb concentrations observed in recent public health incidences. Specifically, the maximum allowed level of Pb in water is 15 ppb as set by EPA. Higher Pb concentrations have been recently reported in several public health incidence related to Pb exposure (Triantafyllidou et al., 2009, 2013) Furthermore, U.S. Center for Disease Control and Prevention has recommended BLL of 5 $\mu g/dL$ (50 ppb) in children as the action level that requires medical attention.

We started by examining the effects of selected Pb concentrations on cell viability and morphology. After 96 h of treatment, the selected Pb doses were found to have minimal effects on cell viability (Fig. 1B) and morphology, including nuclear size, eccentricity which measures the ratio of major and minor axis (the eccentricity of a circle equals to zero) and extent which quantifies the irregularity of a nucleus (protrusions result in larger values of extent) (Figs. S1A-C, (Supporting Information)) consistent with previous literature reports suggesting low doses of Pb (<1 $\mu M \cong 207$ ppb) have minimal effects on cell viability and phenotype (Crumpton et al., 2001; Deng et al., 2001).

Pb was then removed from culture medium by washing three times with PBS before starting differentiation. SH-SY5Y cells can be differentiated into neuron-like cells that stain positive for MAP2 (see Fig. 1C and S2A (Supporting Information)), a neuron-specific protein that is essential for neurogenesis (Teng et al., 2001; Chilton and Gordon-Weeks, 2007). In unexposed cells, ~75% of cells are found to be MAP2 positive (MAP2+%) (Fig. S2B, Supporting Information), which is in a close accordance with literature reports suggesting the SH-SY5Y cells can be used as a model system to study neuronal differentiation (Dwane et al., 2013). Exposure to Pb can reduce MAP2+% particularly at 15 ppb as shown in Fig. S2B (Supporting Information). Although decrease in mean values are

observed at 50 ppb compared to the control, the decrease was not found to be statistically significant. We subsequently quantified MAP2 expression as MAP2 staining intensity per cell. As shown in Fig. 1D, MAP2 intensity was significantly reduced after exposure to Pb. Quantitatively MAP2 intensity was reduced by ~30 and 10% after exposure to 15 and 50 ppb of Pb, respectively as shown in Fig. 1D.

Neurite outgrowth is an important characteristic of neuron that can be typically measured by neurite length and complexity. Neurite length was thus measured via ImageJ as shown in Fig. S2C (Supporting Information) and summarized in Fig. 1E. Exposure to Pb has resulted in longer neurite length at both 15 and 50 ppb but with seemingly reduced level of complexity as shown in Fig. S2D (Supporting Information).

Nuclear morphology, including nucleus area, eccentricity and extent of differentiated neurons were determined as described previously as shown in Figs. S1D-F (Supporting Information). After the completion of differentiation, significant changes were observed in nucleus area and extent, suggesting the potential attenuation of exposure effects through differentiation.

3.2. Low-dose of Pb exposure results in significant acute changes in epigenome

Epigenetic changes consist primarily of DNA methylation and histone post-translational modifications. Compared to active epigenetic markers, i.e., histone acetylation, repressive epigenetic marks, such as DNA methylation (methylation of cytosine in particular), H3K9me3 and H3K27me3 are crucial for forming transcriptionally repressed regions essential for cell lineage determination (Hawkins et al., 2010; Becker et al., 2016) and tend to persist over time. We thus evaluated immediate changes in these repressive markers after Pb exposure.

SH-SY5Y cells were exposed to Pb for 96 h, washed, fixed and immuno-stained for the selected epigenetic modifications, including 5 mC, H3K9me3 and H3K27me3 as shown in Fig. 2A—C. More images of immuno-stained cells can be found in Figs. S3A, D and G (Supporting Information). After exposure, undifferentiated SH-SY5Y cells stained with 5 mC antibodies exhibit small islands enriched in 5 mC as bright foci. Changes in 5 mC can be quantified via Integrated Intensity per Nucleus (IIN) as established in literature (Kageyama et al., 2007; Ramsawhook et al., 2017; Stefanovski et al., 2017). Upon visual inspection, Pb treatment does not seem to immediately elicit significant changes in 5 mC patterns. Analysis of IIN, however, suggests that Pb treatment can lead to ~12.3 and 8.5% reduction in 5 mC levels for 15 and 50 ppb treated SH-SY5Y cells as shown in Fig. 2D.

A more in-depth pattern analysis was then carried out by identifying cell nucleus followed by determining foci features using a customized CellProfiler pipeline, as we detailed in our previous work (Sánchez et al., 2019). Representative images showing nucleus and foci identification via our pipeline for 5 mC-stained images are shown in Fig. S4A and B (Supporting Information). To highlight changes in 5 mC patterns due to Pb exposure, we included only texture features in our clustering analysis (all intensity and shape related features were omitted in constructing the principal component space). A PCA plot illustrating the separations of all treated groups are shown in Fig. 2G. No good separation is observed among differently treated cells suggesting no significant texture changes consistent with our visual observations.

RT-qPCR was then performed to determine changes in epigenetic enzymes that modulate 5 mC levels in cells. Table S3 (Supporting **Information**) summarizes our qPCR results. Relative changes in the mRNA levels of DNA methyltransferase, including DNMT1, DNMT3A, and DNMT3B, and DNA demethylase TET1 are

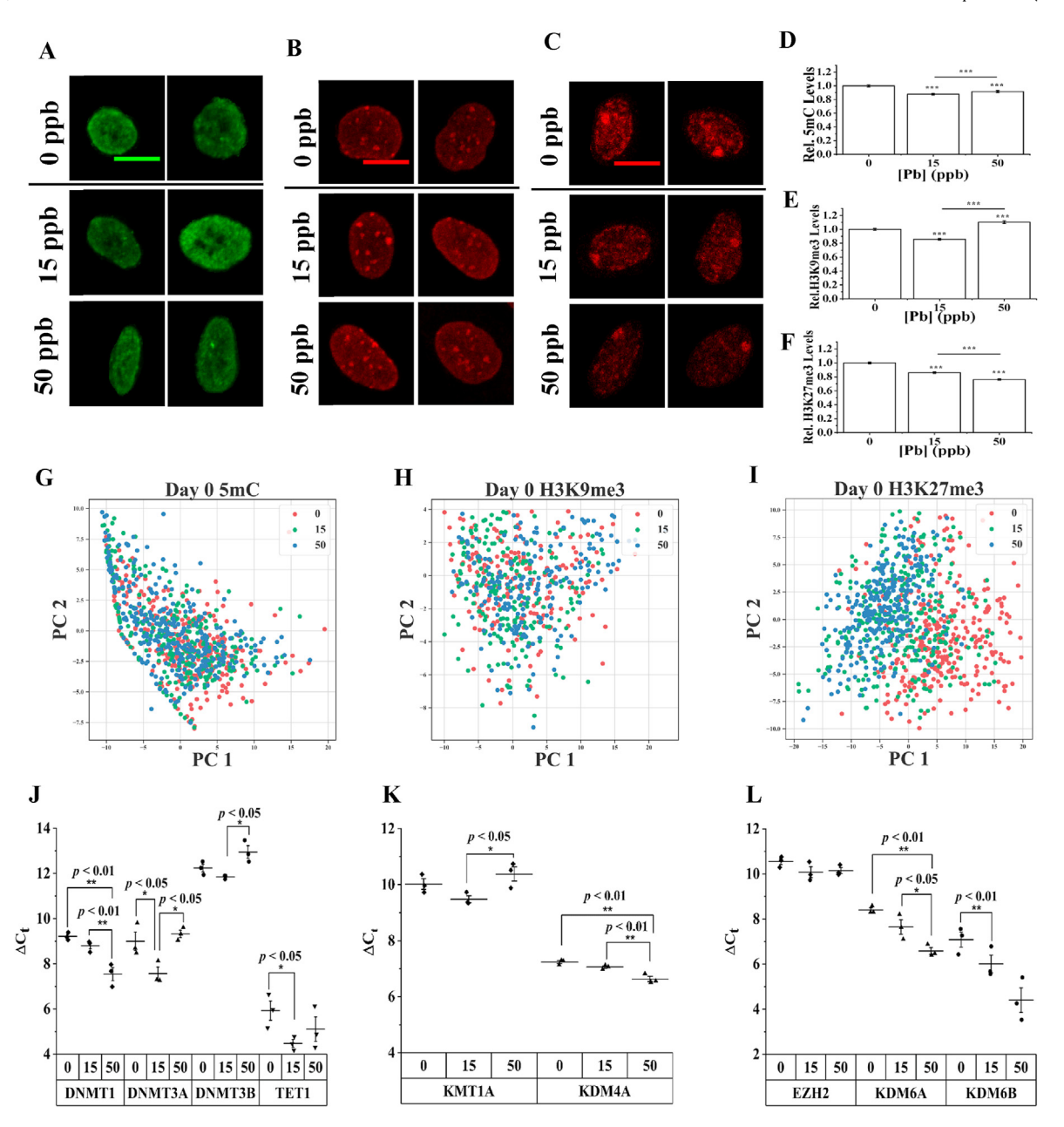


Fig. 2. (A–C) 2D stacked confocal images of undifferentiated SH-SY5Y cells stained for **(A)** 5 mC, **(B)** H3K9me3, and **(C)** H3K27me3 after 96 h exposure to Pb of varying doses. Scale bar = 10 μm. **(D–F)** Relative changes in epigenetic modifications, namely **(D)** 5 mC, **(E)** H3K9me3 and **(F)** H3K27me3 after exposing to Pb of varying doses. Data = mean \pm standard error. n > 500 cells. ***[=] p < 0.001. **(G–I)** Principal component analysis of texture features. Principal component 1 and 2 (PC1 and PC2, respectively) were selected as the axes explaining most of the data variance. **(G)** 5 mC, **(H)** H3K27me3. **(J–L)** Expression levels of mRNA coding for epigenetic writer and erasers, assessed immediately after 96 h of exposure to Pb. Data are presented as the mean difference in cycle threshold (Ct) between gene of interest and β-actin. Error bars represent standard deviation. **(J)**. Enzymes responsible for 5 mC, namely DNMT1, DNMT3A, DNMT3B, and TET1. **(K)**. Enzymes that are highly specific for H3K9me3, namely KMT1A and KDM4A. **(L)**. Enzymes that are highly specific for H3K27me3, namely EZH2, KDM6A and KDM6B. Data = mean \pm standard deviation. n > 3. * [=] p < 0.05, ** [=] p < 0.01.

shown in Fig. 2J. Pb treatments significantly upregulate the transcription level of DNMT3A (*de novo* DNA methyltransferase) and TET1 at 15 ppb, and DNMT1 (maintenance DNMT) at 50 ppb with respect to the control, having fold changes in the gene expression of DNMT3A, DNMT1 and TET1 of 2.79, 3.32, and 2.78, respectively. In addition, within Pb treatments the transcription level of DNMT1, DNMT3A, and DNMT3B (*de novo* DNA methyltransferase) presented significant difference. The increment of Pb concentration from 15 ppb to 50 ppb thus caused an upregulation in DNMT1, while DNMT3A and DNMT3B were downregulated. These results can partially explain the obtained changes in 5 mC during Pb exposure. Similar analysis was performed for H3K9me3 and H3K27me3

stained cells. Briefly, H3K9me3 form larger and more distinctive clusters compared to 5 mC. These clusters are enriched within cell nucleus marking constitutive heterochromatin regions as well as in the perinuclear region marking laminin-associated domains as shown in Fig. 2B and S3D (Supporting Information). Intensity analysis suggests ~12.3% reduction and 10.4% increase in H3K9me3 levels for cells exposed to 15 and 50 ppb of Pb, respectively as shown in Fig. 2E. Visual inspection of stained cells does not suggest any significant pattern changes. PCA analysis was performed using identified cluster features (see also Fig. S4C (Supporting Information)) as shown in Fig. 2H. Cells with different treatments are not distinguishable within the PC space suggesting no significant

pattern changes. Fig. 2K summarizes changes in H3K9me3 writer (KMT1A) and eraser (KDM4A). Relative to the untreated control, Pb treatment mainly affects the transcription level of KDM4A, increasing its gene expression level by 1.52-fold at 50 ppb. Within Pb treatment groups, increasing the Pb concentration from 15 to 50 ppb causes a significant reduction in the mRNA level of KMT1A while the mRNA level of KDM4A was increased. The observed changes in epigenetic enzymes cannot account for the observed changes in H3K9me3 resulting from 15 ppb treatment.

H3K27me3-stained cells exhibit a bright locus near the nucleus periphery, corresponding to barr body found in female origin cells, i.e., SH-SY5Y, representing inactive X chromosome (Chadwick and Willard, 2004; Shenoda et al., 2018). Small foci enriched in H3K27me3 features are also found primarily within cell nucleus but also in the periphery regions as shown in Fig. 2C and S3G (Supporting Information). Intensity analysis of exposed cells revealed ~13.9 and 23.8% reduction in H3K27me3 levels for 15 and 50 ppb treatments, respectively as shown in Fig. 2F. Texture features from the segmented nucleus and foci (Fig. S4D) were compiled and analyzed using PCA as shown in Fig. 2I. Visual inspection of the plot suggests potential separations of Pb-naïve and treated cells, but the distinctions are not sufficient to form distinctive clusters using K-means clustering approach. RT-qPCR was then performed to assess changes in H3K27me3 writer (i.e., EZH2) and erasers (i.e., KDM6A and KDM6B) as shown in Fig. 2L. Relative to the control, exposure to 50 ppb of Pb increased the transcription level of KDM6A and KDM6B by ~3.6 and 6.6 folds, respectively. Within Pb treatments, mRNA levels for KDM6A significantly increased from 15 to 50 ppb. Conversely, no statistical difference was observed between the control and Pb treated groups for mRNA levels of EZH2. The observed changed in the expression of epigenetic enzymes can thus at least partially account for the observed changes in H3K27me3 after Pb exposure.

3.3. Epigenome changes remain in exposed SH-SY5Y cells after cessation of exposure and completion of differentiation

Pb was removed from SH-SY5Y cell culture prior to initiating the differentiation protocol. Differentiation was completed on Day 14 and cells were fixed followed by immuno-staining for 5 mC, H3K27me3 or H3K9me3 then. Typical images of postdifferentiation neurons are shown in Fig. 3A-C and S3B, E, and H (Supporting Information). Significant intensity changes are still observed among different treatment groups and were compared to immediately after exposure to Pb (Day 0) as summarized in Fig. 3D-F. Briefly, after differentiation, changes in 5 mC are further amplified with a decrease in 5 mC levels of ~55.1 and 46.4% for 15 ppb and 50 ppb treatment groups respectively (Fig. 3D). The difference, however, is less discernible within Pb-treated groups. PCA analysis was carried out using texture features as shown in Fig. 3G. The texture features of 5 mC enable separations between Pb-naïve and treated groups after the removal of Pb and completion of differentiation. Two major clusters can be identified via Silhouette plot (Rousseeuw, 1987) followed by k-means clustering (Lloyd, 1982). Cluster 1 contains primarily untreated cells (~73%) while Cluster 2 consists mainly of Pb-treated SH-SY5Y cells (~87%) as shown in Fig. S5A (Supporting Information). The contributions of texture features were rank ordered via a Lasso analysis (Tibshirani, 2011). Among the top 5 contributors as summarized in Fig. S5B (Supporting Information), entropy features of 5 mC within a nucleus and texture features of each 5 mC island (foci) were ranked the highest, suggesting association of significant arrangement of 5 mC loci within a nucleus.

Different from changes in 5 mC, alterations in H3K9me3 and H3K27me3 are compensated and (partially) recovered after the

completion of differentiation. Specifically, H3K9me3 level was increased by ~58.9 and 56.0%, respectively as compared to the untreated group in contrast to a global decrease right after exposure to Pb (Fig. 3E). Other than intensity, no significant texture changes are observed among treatment and control groups (Fig. 3H). Differentiated SH-SY5Y cells exhibit ~19.4 and 11.4% decrease in H3K27me3 levels from pre-differentiation exposure to 15 and 50 ppb of Pb, respectively (Fig. 3F). The decrease in H3K27me3 levels was amplified for 15 ppb treated cells while a partial recovery was observed by cells exposed to 50 ppb contrasting to immediately after exposure (Fig. 3F). Texture analysis as shown in Fig. 3I does not suggest any significant alterations in H3K27me3 distributions within cell nucleus.

3.4. Differentiation as a potential confounding factor in propagating epigenetic memory

Systematic epigenome reprogramming is known to take place during differentiation leading to potential confounding effects (Li, 2002; Tibshirani, 2011). To understand this, control experiments were carried out as illustrated in Fig. 4A. Briefly, instead of starting differentiation right after exposure, SH-SY5Y cells were rinsed three times with PBS and continuously cultured in a Pb-free culture medium after cessation of exposure to Pb. Typical immuno-stained images for 5 mC, H3K9me3 and H3K27me3 were summarized in Fig. 4B–D with more images in Fig. S3 C, F and I (Supporting Information). Compared to this undifferentiated control, differentiation clearly resulted in significant increases in all selected repressive markers, namely 5 mC, H3K9me3 and H3K27me3 levels as shown in Fig. 3D–F potentially as a result of heterochromatin establishment in the untreated control.

After cessation of exposure to Pb for 14 days, other than 5 mC, changes in H3K9me3 and H3K27me3 are both compensated for as summarized in Fig. 4E-G. Specifically, changes in 5 mC after exposure to Pb are retained and amplified after 14 days. The magnitude in changes (~22.2 and 31.9% for 15 and 50 ppb of Pb, respectively), however, is much smaller compared to cells undergoing differentiation (~55.1 and 46.4% for 15 and 50 ppb of Pb, respectively) as shown in Fig. 4E. Changes in H3K9me3 are partially recovered after 14 days in continuously cultured SH-SY5Y cells (No statistical significance observed for 15 ppb, and ~7% increase for 50 ppb), while they were overcompensated in differentiated SH-SY5Y cells (see Fig. 4F). Surprisingly, in continuously cultured SH-SY5Y cells, changes in H3K27me3 are overcompensated (~19.7 and 49.4% for 15 and 50 ppb of Pb, respectively), which exhibit a trend opposite to differentiated cells. Texture analysis was carried out similarly as described in the previous sections with results summarized in Fig. 4H-J. While the 5 mC, H3K9me3 H3K27me3 intensity levels of treated groups demonstrate significant difference from untreated controls, we cannot distinguish between Pbnaïve and treated groups based on their underlying texture

Changes in nuclear morphology of continuously cultured SH-SY5Y cells were also assessed as described for undifferentiated and differentiated cells previously. No significant changes were observed between Pb-naïve and treated groups as shown in Figs. S1G-I (Supporting Information).

4. Discussion

4.1. Exposure to low dose of Pb elicits immediate changes in gene repressive markers

We selected to work with low doses of Pb (15 and 50 ppb) because of their relative high incidence of exposure (Hauptman

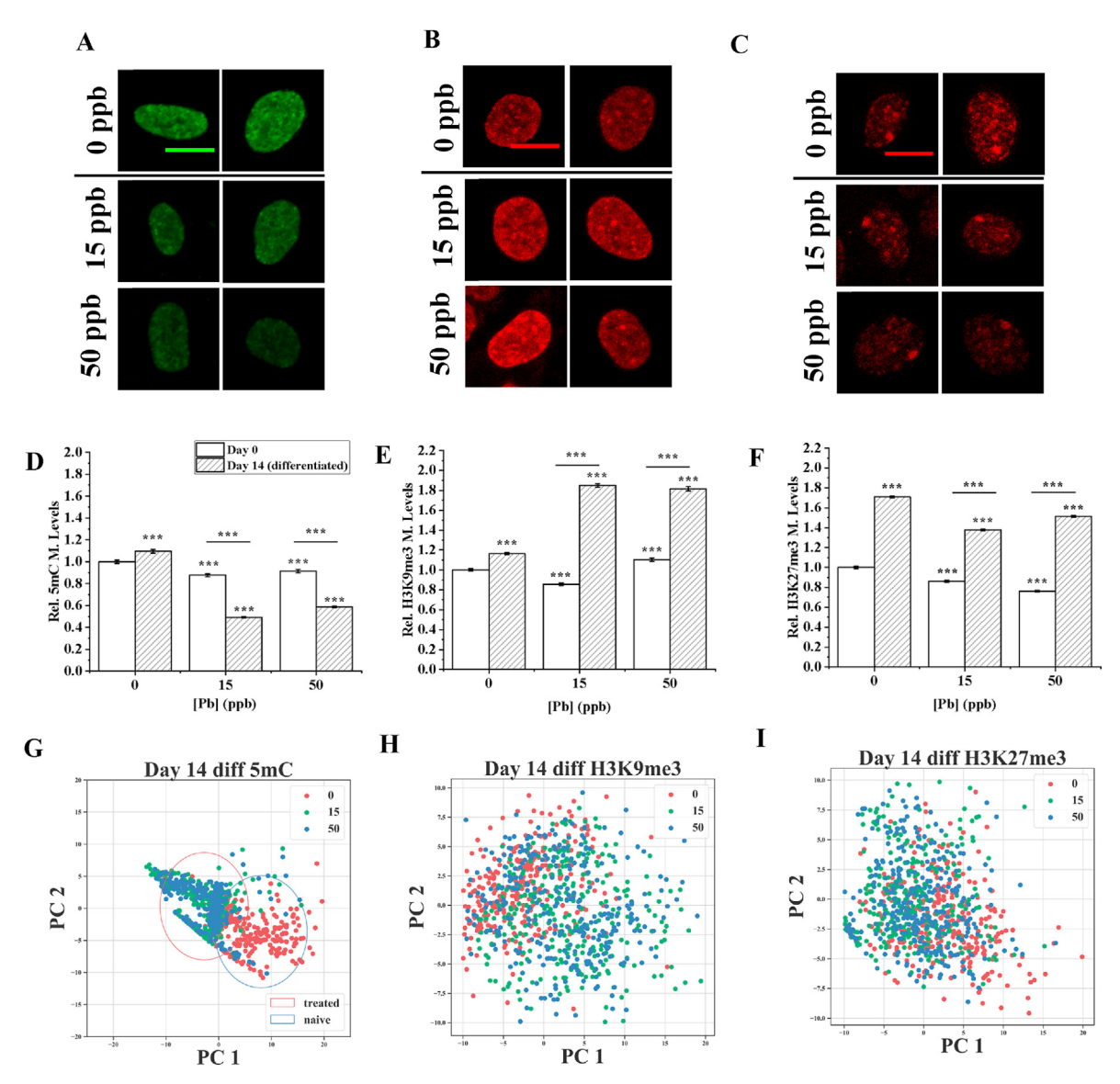


Fig. 3. (A–C) 2D stacked confocal images of SH-SY5Y cells stained for **(A)** 5 mC, **(B)** H3K9me3, and **(C)** H3K27me3 after 96 h exposure to Pb, removal of Pb by medium swapping and completion of differentiation. Scale bar = 10 μ m. **(D–F)** Relative changes in epigenetic modifications, namely **(D)** 5 mC, **(E)** H3K9me3 and **(F)** H3K27me3 after exposing to Pb of varying doses on Day 0 and Day 14 (after differentiation). All data are normalized to fluorescent intensity of untreated cells observed on Day 0. Data = mean \pm standard error. n > 500 cells. ***[=] p < 0.001. **(G–I)** Principal component analysis of image pattern features. Principal component 1 and 2 (PC1 and PC2, respectively) were selected as the axes explaining most of the data variance. **(G)** 5 mC, **(H)** H3K9me3, **(I)** H3K27me3.

et al., 2017; Lanphear et al., 2018) as well as increasing concerns of exposure-affiliated long-term neurodegenerative diseases in later life (Shefa and Héroux, 2017; Bellinger et al., 2018). Exposure of SH-SY5Y cells to the selected doses of Pb for 96 h do not elicit significant phenotypic changes in cells, including metabolic and morphological properties consistent with previous literature findings (Crumpton et al., 2001; Deng et al., 2001).

Meanwhile, significant changes are observed in selected epigenetic markers, namely 5 mC, H3K9me3 and H3K27me3. 5 mC is the most abundant epigenetic changes occurring on DNA and has an established role in gene regulation (Cedar and Razin, 2017; Kribelbauer et al., 2017). Exposure to Pb resulted in larger reductions in 5 mC at 15 ppb compared to cells exposed to 50 ppb of Pb suggesting non-linear dependence in Pb doses. The acute 5 mC changes occur globally with no significant pattern changes observed within cell nucleus right after exposure. Changes in the expression of 5 mC writer and eraser enzymes are also observed

with an overall increase in both writer and eraser enzyme expression at 15 ppb and dominate changes only in 5 mC writer enzymes at 50 ppb. The expression level changes of these epigenetic enzymes can thus partially explain the observed 5 mC changes. Other factors, such as altered epigenetic enzyme activities as demonstrated in literature (Sanchez et al., 2017) may also contribute to the observed changes.

5 mC is the most abundant DNA epigenetic modification and a common repressive marker found in silenced chromatin. 5 mC plays an important role during cell differentiation by modulating the expression of developmental genes and defining cell lineages (Hochedlinger and Plath, 2009). Precise temporal control of DNA methylation profiles is crucial for the differentiation and maturation of the nervous system. Studies have demonstrated that the timing of DNA methylation on the promoter of specific genes, for example fibrillary acidic protein (Gfap) gene can affect lineage commitment in neural precursor cells and result in preference for

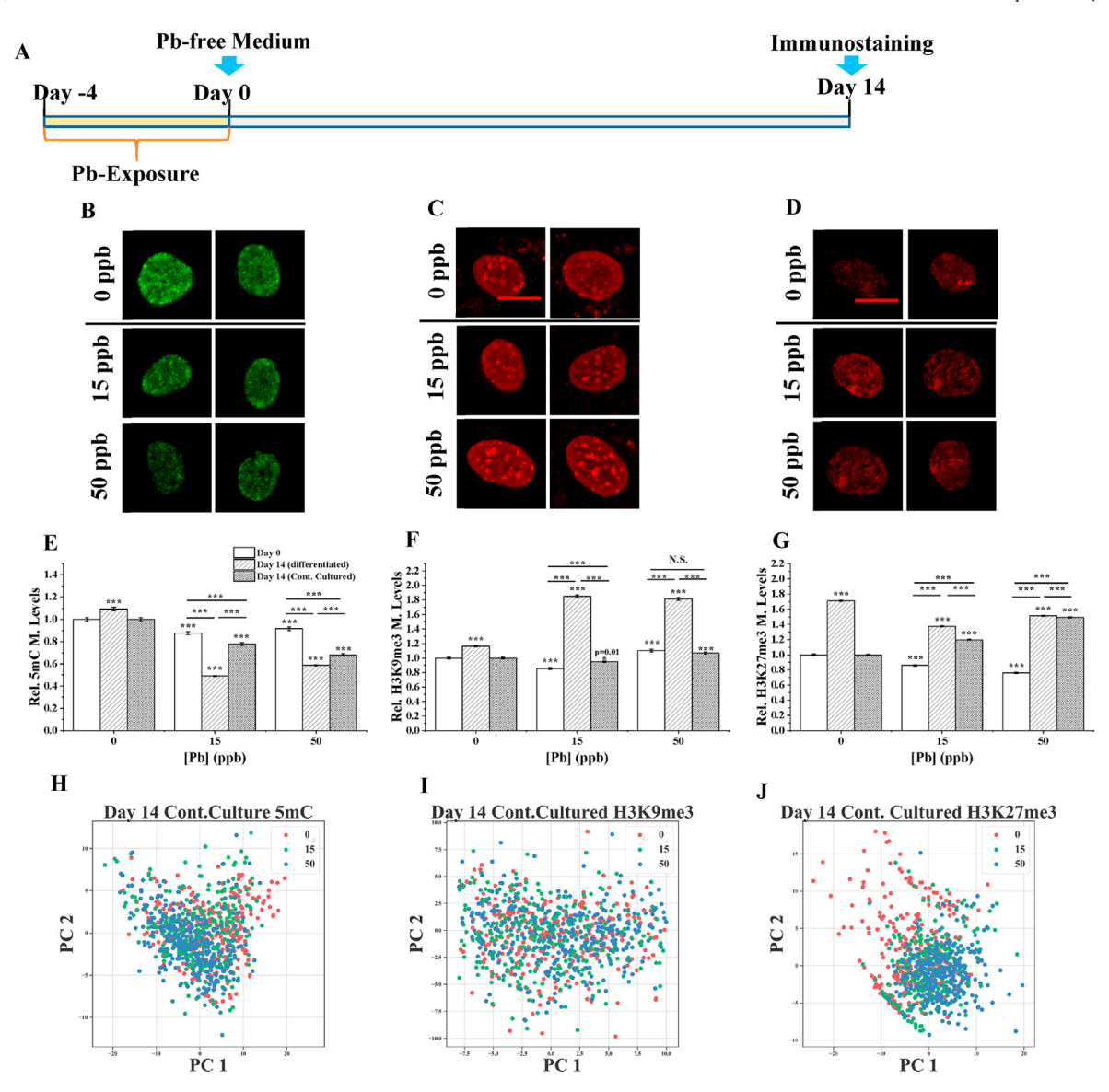


Fig. 4. (A) A schematic illustration of the exposure and continuous culturing timeline for SH-SY5Y cells. (**B-D**) 2D projected immunostaining images of Pb exposed SH-SY5Y cells relaxed in Pb-free medium for 14 days (**B**) 5 mC, (**C**) H3K9me3, (**D**) H3K27me3. Scale bar = 10 μ m. (**E**–**F**) Bar graph demonstrating the relative changes in epigenetic modifications, (**E**) 5 mC, (**F**) H3K9me3 and (**G**) H3K27me, after exposure to Pb²⁺ quantified at different time and conditions: day 0, day 14 with differentiation, and day 14 without differentiation. All data are normalized to fluorescent intensity of untreated cells observed on Day 0. Data are represented as mean \pm standard error. n > 500 cells. Asterisks above the column indicate significance relative to the control, N.S.: no significance (p > 0.05), ***[=] p < 0.001, (H–J) Principal component analysis for image pattern features after continuous culturing. Principal component 1 and 2 (PC1 and PC2, respectively) were selected as the axes explaining most of the data variance. (**H**) 5 mC, (**I**) H3K9me3, (**J**) H3K27me3.

astrocytic lineages (Moore et al., 2013). Exposure to low dose of Pb has been shown to alter DNA methylation level in several animal studies, including zebrafish (Sanchez et al., 2017), rat (Sun et al., 2017; Singh et al., 2018a) and human cell lines (Li et al., 2011; Nye et al., 2015). The observed nonlinear dose-response is not uncommon. For example, in a recent rat study researchers have found that a significant larger number of genes are differentially methylated after exposure to low dose of Pb at 150 ppm as compared to 375 ppm (Singh et al., 2018b).

H3K9me3 and H3K27me3 are both suppressive markers typically found in transcriptionally silent chromatin regions. H3K9me3 are particularly enriched in constitutive heterochromatin that are almost permanently turned off (Becker et al., 2016). H3K27me3, on the other hand, is enriched in facultative heterochromatin that are suppressed and poised for potential activation (Richards and Elgin, 2002). Both H3K9me3 and H3K27me3 play an important role

during differentiation (Tan et al., 2012; Tyssowski et al., 2014; Yao et al., 2016). For instance, protein-coding genes in an early stage, undifferentiated cells at germ-layer, exhibit high levels of H3K9me3 located mainly in gene bodies, promoters, and termination transcription sites that is reduced upon differentiation (Nicetto et al., 2019). The proper establishment of constitutive heterochromatin is relevant for preventing cell reprogramming and silencing undesirable lineage-specific genes to preserve cellular identity (Becker et al., 2016). H3K27me3 is more evenly distributed over genes and intragenic regions in differentiated cells and is reduced significantly during cell differentiation (Nicetto et al., 2019). Moreover, changes in H3K9me3 and H3K27me3 are known to be potentially persistent and inheritable across generations (Zenk et al., 2017; Perez and Lehner, 2019) warranting detailed study in this work. Global reduction in H3K9me3 level is observed at 15 ppb while a slight increase is observed at 50 ppb, mirroring

discoveries in 5 mC and suggesting a non-linear dose dependence. Although changes are observed in H3K9me3 writer and erase enzymes, the observed changes cannot explain the alterations in H3K9me3 levels. SH-SY5Y cells exposed to Pb exhibit significant reductions in H3K27me3 levels (with 13.9 and 23.8% for 15 and 50 ppb respectively). Significant increase is observed in the transcriptional level of H3K27me3 erasers, namely KDM6A and KDM6B providing a plausible explanation to the observed global changes in H3K27me3.

Limited studies exist examining the effects of Pb-exposure on histone modifications. A mouse study suggests that prenatal exposure to Pb of 100 ppm, where pups were continuous exposed to Pb from gestation to lactation, can reduce H3K9me3 level in the cortex of female and male rats by 49 and 65%, respectively (Schneider et al., 2016). Similar trend was recapitulated in our cell culture study using undifferentiated SY5Y cells. The observed changes in H3K9me3 seemingly mirror changes in 5 mC at different Pb doses, suggesting a potential cross-talking between DNA methylation and H3K9me3, which has been suggested in literature (Du et al., 2015; Zhao et al., 2016) and observed in our previous work of human cells exposed to atrazine (Sánchez et al., 2020).

Exposure to Pb (5 μ M \cong 1035 ppb) has been reported to result in ~30% reductions in H3K27me3 at hippocampal neurons from rats (Gu et al., 2019). Similar reductions in H3K27me3 were also observed in hippocampus of female rats with chronic exposure to Pb of 125 ppm (Xiao et al., 2020). Our observations in SH-SY5Y cells are thus consistent with literature findings and thus can be plausibly explained by increase in the transcriptional level of H3K27me3 erasers.

4.2. Long-term epigenome changes with and without differentiation

Different from genetic mutations that are irreversible in nature, epigenetic changes are dynamic and thus potentially reversible. The dynamic balance of an epigenetic change is typically modulated by the presence of epigenetic writer and eraser enzyme. Most exposures to environmental chemicals are for a short duration of time. Assessing the persistence of acquired epigenome changes after cessation of exposure is thus critically important to understand their potential roles in long-term health. Here, we considered two different scenarios after cessation of exposure, namely through continuous culturing and via a neuron-specific differentiation. Changes persists in both cases while details vary depending on the type of modification and culturing methods.

After cessation of exposure, continuously cultured cells maintain its lower 5 mC level compared to the untreated control and the changes are seemingly amplified after 14 days. Differentiation further amplifies the difference in 5 mC levels among our experimental groups. In addition to global intensity changes, significant alterations in 5 mC distribution patterns are also determined via texture analysis. After differentiation, untreated cells have significantly increased 5 mC levels with more distinctive 5 mC-enriched islands established within the cell nucleus. A more random and diffusive pattern, however, is observed in treated cells suggesting less well-defined heterochromatin regions separated by distinctive 5 mC levels.

Different from 5 mC, cells try to compensate for the loss in both H3K9me3 and H3K27me3 levels after removal of Pb with and without differentiation. H3K9me3 level is almost completely restored and becomes almost indistinguishable from the untreated group after 14 days of continuous culturing. With differentiation, significant increase in H3K9me3 is observed suggesting an overall upregulation in H3K9me3 likely prompted by homeostasis and differentiation driving forces. Changes in H3K27me3 are also

compensated in both continuous culturing and differentiation experiments. The compensation, however, is more significant in continuously cultured cells resulting in an increase in H3K27me3 levels after 14 days, while differentiated SH-SY5Y cells with prior exposure to Pb becomes more like their untreated counterparts.

Since 5 mC, H3K9me3 and H3K27me3 all tag silenced chromatin, we compared the correlation of the observed changes in the selected marks as summarized in Figs. S6A-C (Supporting Information). The correlation coefficients between different pairs were summarized in Fig. S6D (Supporting Information). On Day 0 after acute Pb exposure, all marks exhibit a weak correlation in between (Pearson's coefficient = 0.390, 0.740 and -0.331 for 5mc-H3K9me3, 5mc-H3K27me3 and H3K9me3-H3K27me3) suggesting potentially unique response mechanism to Pb-exposure. Strong correlations, however, were observed after 14 days upon the completion of differentiation in all pairs. A strong positive correlation was observed between 5 mC and H3K27me3 (Pearson's coefficient = 0.962). Strong negative correlations were observed in 5 mC-H3K9me3 and H3K9me3-H3K27me3 pairs. In contrast, a strong negative correlation was only observed between 5 mC and H3K27me3 after 14 days of continuous culturing. Our results thus suggest that silencing markers, although may not be modulated via similar upstream regulators can have concerted changes after completion of cell differentiation as a result of required synergistic modulation of various repressive markers during lineage commitment.

Accompanying the observed epigenome changes, we also noted significant alterations in nuclear size and morphology as summarized in Fig. S1 (Supporting Information) only in differentiated cells treated with Pb. After exposure, differentiated neurons exhibit larger nucleus area relative to their untreated counterparts. Nuclear eccentricity that measures the roundness of cells were not significantly altered. Nuclear extent which quantifies shape irregularity was also found to be significantly altered after Pb exposure. The absence of nuclear alteration in continuously cultured cells further suggests a potential compounding effect of neuronal differentiation on Pb exposure effects. Neurite length difference was also observed in differentiated SH-SY5Y cells after exposure to Pb with increased neurite length and reduced complexity. This finding suggests that neurite outgrowth was potentially impaired in differentiated neurons after exposure to Pb. This is consistent with previous study using PC12 cells suggesting Pb-treated PC12 cells can demonstrate enhanced neurite outgrowth (Crumpton et al., 2001; Davidovics and DiCicco-Bloom, 2005). Furthermore, exposed SH-SY5Y cells have lower neuron differentiation efficiency featuring fewer MAP2+% cells and lower MAP2 expression. MAP2 expression levels is commonly associated with the stability of neuroarchitecture. We thus correlated changes in the observed phenotypic features (MAP2 expression and Neurite length) with Pb doses as shown in Fig. 5. Similar correlations were also performed using 5 mC and Pb doses. A strong positive correlation was observed between the phenotypic alterations and 5 mC changes (Pearson's correlation coefficient = 0.9998 and 0.9891 for MAP2 expression and neurite length, respectively) suggesting a potential underlying correlative/ causative relationship.

Persistent changes in 5 mC after exposure to Pb have been reported in PC12 cells using Pb doses of 50 (10.35 ppb), 250 (51.71 ppb), and 500 nM (103.5 ppb) (Li et al., 2012). Cynomolgus monkeys with Pb exposure at infancy was found to exhibit impaired DNMT activities (~20% reductions in activity) in brain tissue 23 years after exposure (Wu et al., 2008). Our observations are thus consistent with previous literature reports. To the best of our knowledge, no studies have evaluated the persistency of H3K9me3 and H3K27me3 marks after cessation of Pb exposure.

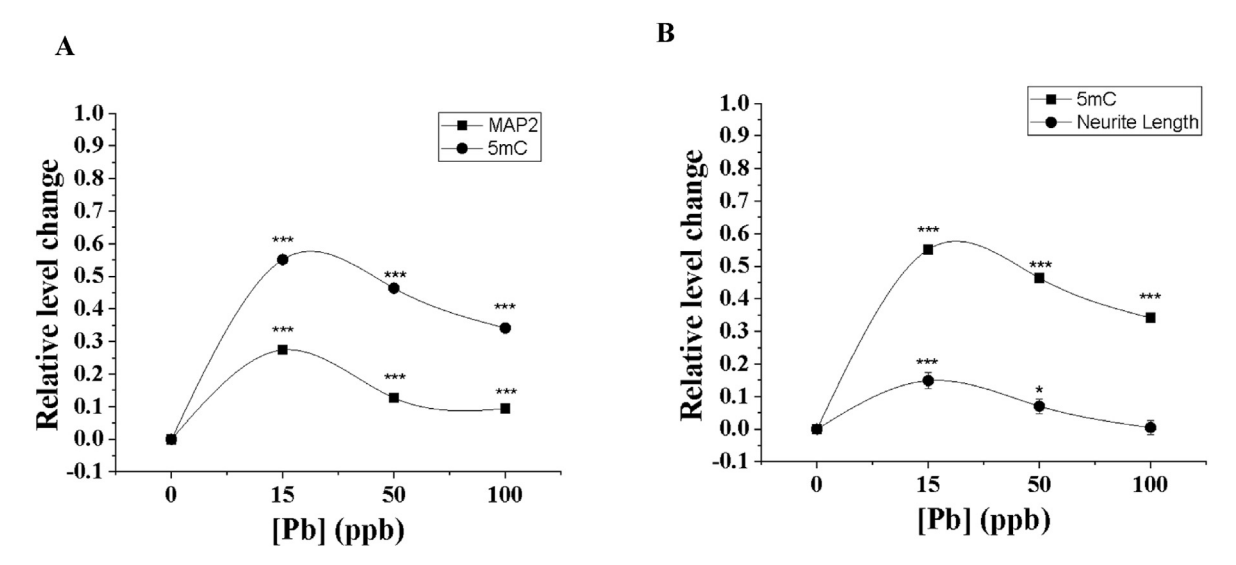


Fig. 5. (A) Relative trends of changes in 5 mC modification levels and MAP2 expressions on Day 14. Trends are positively correlated (Pearson's correlation = 0.9998). **(B)** Relative trends of changes in 5 mC modification levels and Neurite length on Day 14. Trends are positively correlated (Pearson's correlation = 0.9891). A treatment concentration of 100 ppb was added to enhance statistical power. 5 mC modification levels, neurite length and MAP2 expression levels were quantified as described above. All data are normalized to untreated group. Data = Mean \pm S.E. n > 500 cells. *** | p < 0.001.

5. Conclusions

Collectively, exposure to low doses of Pb can alter 5 mC levels which can persist and attenuate through time and differentiation. Changes in histone repressive markers, H3K9me3 and H3K27me3 are both compensated for during continuous culturing and differentiation. Over-compensations, however, are observed for H3K9me3 during differentiation and H3K27me3 during continuous culturing. Although no phenotypic changes are observed immediately after Pb exposure, significant alterations are observed in the ability of differentiation (MAP2+%), neuron stability (MAP2 level), neurite outgrowth (neurite length) and neurite complexity after Pb exposure prior to differentiation. Dose-dependent phenotypic changes seem to correlate well with alterations in 5 mC levels. Taken together, our results unequivocally suggest that exposure to low dose of Pb, particularly prior to differentiation, can result in persistent changes in epigenome that last after the cessation of Pb exposure and potentially contribute to the observed phenotypic changes with implications in long-term health.

Author contribution

Li Lin: Conceptualization, Methodology, Experiment, Data curation, Writing- Reviewing and Editing, Junkai Xie: Methodology, Experiment and Reviewing, Oscar Sanchez: Methodology, Writing-Reviewing and Editing, Chris Bryan: Visulaization and Analysis, Jennifer Freeman: Conceptualization, Methodology and Reviewing, Chongli Yuan: Conceptualization, Methodology, Writing- Reviewing, Editing and Supervising.

Funding

This work was supported by National Science Foundation [CBET-1512285, CBET-1705560 & EF-1935226].

Declaration of competing interest

The authors declare that they have no known competing financial interests or personal relationships that could have appeared to influence the work reported in this paper.

Appendix A. Supplementary data

Supplementary data to this article can be found online at https://doi.org/10.1016/j.chemosphere.2020.128486.

References

Annest, J.L., Pirkle, J.L., Makuc, D., Neese, J.W., Bayse, D.D., Kovar, M.G., 1983. Chronological trend in blood lead levels between 1976 and 1980. N. Engl. J. Med. 308, 1373—1377

Becker, J.S., Nicetto, D., Zaret, K.S., 2016. H3K9me3-Dependent heterochromatin: barrier to cell fate changes. Trends Genet. 32, 29–41.

Bellinger, D., Leviton, A., Waternaux, C., Needleman, H., Rabinowitz, M., 1987. Longitudinal analyses of prenatal and postnatal lead exposure and early cognitive development. N. Engl. J. Med. 316, 1037—1043.

Bellinger, D.C., Stiles, K.M., Needleman, H.L., 1992. Low-level lead exposure, intelligence and academic achievement: a long-term follow-up study. Pediatrics 90, 855–861.

Bellinger, D.C., Malin, A., Wright, R.O., 2018. The neurodevelopmental toxicity of lead: history, epidemiology, and public health implications. Advances in Neurotoxicology 1–26. Elsevier.

Bihaqi, S.W., Eid, A., Zawia, N.H., 2017. Lead exposure and tau hyperphosphorylation: an in vitro study. Neurotoxicology 62, 218–223.

Bustin, S.A., Benes, V., Garson, J.A., Hellemans, J., Huggett, J., Kubista, M., Mueller, R., Nolan, T., Pfaffl, M.W., Shipley, G.L., Vandesompele, J., Wittwer, C.T., 2009. The MIQE guidelines: Minimum information for publication of quantitative real-time PCR experiments. Clin. Chem. 55, 611–622.

Caudle, W.M., Guillot, T.S., Lazo, C.R., Miller, G.W., 2012. Industrial toxicants and Parkinson's disease. Neurotoxicology 33, 178—188.

Cecil, K.M., Brubaker, C.J., Adler, C.M., Dietrich, K.N., Altaye, M., Egelhoff, J.C., Wessel, S., Elangovan, I., Hornung, R., Jarvis, K., Lanphear, B.P., 2008. Decreased brain volume in adults with childhood lead exposure. PLoS Med. 5.

Cecil, K.M., Dietrich, K.N., Altaye, M., Egelhoff, J.C., Lindquist, D.M., Brubaker, C.J., Lanphear, B.P., 2011. Proton magnetic resonance spectroscopy in adults with childhood lead exposure. Environ. Health Perspect. 119, 403–408.

Cedar, H., Razin, A., 2017. Annotating the genome by DNA methylation. Int. J. Dev. Biol. 61, 137–148.

Chadwick, B.P., Willard, H.F., 2004. Multiple spatially distinct types of facultative heterochromatin on the human inactive X chromosome. Proc. Natl. Acad. Sci. Unit. States Am. 101, 17450–17455.

Chilton, J.K., Gordon-Weeks, P.R., 2007. Role of microtubules and MAPs during neuritogenesis. Intracellular mechanisms for neuritogenesis 57–88. Springer.

Coon, S., Stark, A., Peterson, E., Gloi, A., Kortsha, G., Pounds, J., Chettle, D., Gorell, J., 2006. Whole-body lifetime occupational lead exposure and risk of Parkinson's disease. Environ. Health Perspect. 114, 1872–1876.

Crumpton, T., Atkins, D.S., Zawia, N.H., Barone, S., 2001. Lead exposure in pheochromocytoma (PC12) cells alters neural differentiation and Sp1 DNA-binding. Neurotoxicology 22, 49–62.

Davidovics, Z., DiCicco-Bloom, E., 2005. Moderate lead exposure elicits neurotrophic effects in cerebral cortical precursor cells in culture. J. Neurosci. Res. 80,

- 817-825.
- Deng, W., McKinnon, R.D., Poretz, R.D., 2001. Lead exposure delays the differentiation of oligodendroglial progenitors in vitro. Toxicol. Appl. Pharmacol. 174,
- Dignam, T., Kaufmann, R.B., LeStourgeon, L., Brown, M., 2019. Control of lead sources in the United States, 1970-2017: public health progress and current challenges to eliminating lead exposure. J. Publ. Health Manag. Pract. 25.
- Du, J., Johnson, L.M., Jacobsen, S.E., Patel, D.J., 2015. DNA methylation pathways and their crosstalk with histone methylation, Nat. Rev. Mol. Cell Biol. 16, 519-532.
- Dwane, S., Durack, E., Kiely, P.A., 2013. Optimising parameters for the differentiation of SH-SY5Y cells to study cell adhesion and cell migration. BMC Res. Notes 6. 366
- Eid, A., Bihaqi, S.W., Renehan, W.E., Zawia, N.H., 2016. Developmental lead exposure and lifespan alterations in epigenetic regulators and their correspondence to biomarkers of Alzheimer's disease, Alzheimer's Dementia: Diagnosis, Assessment & Disease Monitoring 2, 123-131.
- Fanti, Z., De-Miguel, F.F., Martinez-Perez, M.E., 2008. A method for semiautomatic tracing and morphological measuring of neurite outgrowth from DIC sequences. In: 2008 30th Annual International Conference of the IEEE Engineering in Medicine and Biology Society, pp. 1196-1199.
- Flora, G., Gupta, D., Tiwari, A., 2012. Toxicity of lead: a review with recent updates. Interdiscipl. Toxicol. 5, 47–58.
- Gu, X., Xu, Y., Xue, W.-Z., Wu, Y., Ye, Z., Xiao, G., Wang, H.-L., 2019. Interplay of miR-137 and EZH2 contributes to the genome-wide redistribution of H3K27me3
- underlying the Pb-induced memory impairment. Cell Death Dis. 10, 671. Hauptman, M., Bruccoleri, R., Woolf, A.D., 2017. An update on childhood lead
- poisoning. Clin. Pediatr. Emerg. Med. 18, 181–192. Hawkins, D.R., Hon, G.C., Lee, L.K., Ngo, Q, Lister, R., Pelizzola, M., Edsall, L.E., Kuan, S., Luu, Y., Klugman, S., Antosiewicz-Bourget, J., Ye, Z., Espinoza, C., Agarwahl, S., Shen, L., Ruotti, V., Wang, W., Stewart, R., Thomson, J.A., Ecker, J.R., Ren, B., 2010. Distinct epigenomic landscapes of pluripotent and lineagecommitted human cells. Cell Stem Cell 6, 479-491.
- Hochedlinger, K., Plath, K., 2009. Epigenetic reprogramming and induced pluripotency. Development 136, 509-523.
- Jarvis, P., Quy, K., Macadam, J., Edwards, M., Smith, M., 2018. Intake of lead (Pb) from tap water of homes with leaded and low lead plumbing systems. Sci. Total Environ. 644, 1346-1356.
- Kageyama, S.-i., Liu, H., Kaneko, N., Ooga, M., Nagata, M., Aoki, F., 2007. Alterations in epigenetic modifications during oocyte growth in mice. Reproduction 133, 85-94.
- Keniry, A., Gearing, L.J., Jansz, N., Liu, J., Holik, A.Z., Hickey, P.F., Kinkel, S.A., Moore, D.L., Breslin, K., Chen, K., Liu, R., Phillips, C., Pakusch, M., Biben, C., Sheridan, J.M., Kile, B.T., Carmichael, C., Ritchie, M.E., Hilton, D.J., Blewitt, M.E., 2016. Setdb1-mediated H3K9 methylation is enriched on the inactive X and
- plays a role in its epigenetic silencing. Epigenet. Chromatin 9, 16. Kim, Y., Ha, E.-H., Park, H., Ha, M., Kim, Y., Hong, Y.-C., Kim, E.-J., Kim, B.-N., 2013. Prenatal lead and cadmium co-exposure and infant neurodevelopment at 6 months of age: the Mothers and Children's Environmental Health (MOCEH) study. Neurotoxicology 35, 15-22.
- Kribelbauer, J.F., Laptenko, O., Chen, S., Martini, G.D., Freed-Pastor, W.A., Prives, C., Mann, R.S., Bussemaker, H.J., 2017. Quantitative analysis of the DNA methylation sensitivity of transcription factor complexes. Cell Rep. 19, 2383-2395.
- Kungulovski, G., Kycia, I., Tamas, R., Jurkowska, R.Z., Kudithipudi, S., Henry, C., Reinhardt, R., Labhart, P., Jeltsch, A., 2014. Application of histone modificationspecific interaction domains as an alternative to antibodies. Genome Res. 24, 1842-1853.
- Lanphear, B.P., Dietrich, K., Auinger, P., Cox, C., 2000. Cognitive deficits associated with blood lead concentrations <10 microg/dL. In: US Children and Adolescents. Public Health Reports (Washington, D.C.: 1974), vol. 115, pp. 521-529.
- Lanphear, B.P., Rauch, S., Auinger, P., Allen, R.W., Hornung, R.W., 2018. Low-level lead exposure and mortality in US adults: a population-based cohort study. The Lancet Public Health 3, e177-e184.
- Lee, J., Peterson, S.M., Freeman, J.L., 2017. Sex-specific characterization and evaluation of the Alzheimer's disease genetic risk factor sorl1 in zebrafish during aging and in the adult brain following a 100 ppb embryonic lead exposure. J. Appl. Toxicol. 37, 400-407.
- Li, E., 2002. Chromatin modification and epigenetic reprogramming in mammalian development. Nat. Rev. Genet. 3, 662-673.
- Li, C., Xu, M., Wang, S., Yang, X., Zhou, S., Zhang, J., Liu, Q., Sun, Y., 2011. Lead exposure suppressed ALAD transcription by increasing methylation level of the promoter CpG islands. Toxicol. Lett. 203, 48-53.
- Li, Y.Y., Chen, T., Wan, Y., Xu, S.q., 2012. Lead exposure in pheochromocytoma cells induces persistent changes in amyloid precursor protein gene methylation patterns. Environ. Toxicol. 27, 495-502.
- Lloyd, S.P., 1982. Least squares quantization in PCM. IEEE Trans. Inf. Theor. 28 (2),
- Mansouri, M.T., Cauli, O., 2009. Motor alterations induced by chronic lead exposure. Environ. Toxicol. Pharmacol. 27, 307-313.
- Meissner, G., 2017. The structural basis of ryanodine receptor ion channel function. J. Gen. Physiol. 149, 1065-1089.
- Meyer, D.N., Crofts, E.J., Akemann, C., Gurdziel, K., Farr, R., Baker, B.B., Weber, D., Baker, T.R., 2020. Developmental exposure to Pb2+ induces transgenerational changes to zebrafish brain transcriptome. Chemosphere 244, 125527.
- Moore, L.D., Le, T., Neuropsychopharmacology, F.-G., 2013. DNA methylation and its basic function. Neuropsychopharmacology 38 (1), 23-38.

Needleman, H., 2004. Lead poisoning. Annu. Rev. Med. 55, 209-222.

- Nevin, R., 2000. How lead exposure relates to temporal changes in IQ, violent crime, and unwed pregnancy. Environ. Res. 83, 1–22.
- Nevin, R., 2007. Understanding international crime trends: the legacy of preschool lead exposure. Environ. Res. 104, 315-336.
- Nicetto, D., Donahue, G., Jain, T., Peng, T., Sidoli, S., Sheng, L., Montavon, T., Becker, J.S., Grindheim, J.M., Blahnik, K., 2019. H3K9me3-heterochromatin loss at protein-coding genes enables developmental lineage specification. Science 363, 294-297.
- Nriagu, J.O., 1990. The rise and fall of leaded gasoline. Sci. Total Environ. 92, 13–28. Mye, M.D., Hoyo, C., Murphy, S.K., 2015. In vitro lead exposure changes DNA methylation and expression of IGF2 and PEG1/MEST. Toxicol. Vitro 29, 544-550.
- Obeng-Gyasi, E., 2019. Sources of lead exposure in various countries. Rev. Environ. Health 34, 25-34.
- Perez, M.F., Lehner, B., 2019. Intergenerational and transgenerational epigenetic inheritance in animals. Nat. Cell Biol. 21, 143–151. Pieper, K.J., Martin, R., Tang, M., Walters, L., Parks, J., Roy, S., Devine, C.,
- Edwards, M.A., 2018. Evaluating water lead levels during the flint water crisis. Environ. Sci. Technol. 52, 8124–8132.
- Ramsawhook, A.H., Lewis, L.C., Eleftheriou, M., Abakir, A., Durczak, P., Markus, R., Rajani, S., Hannan, N.R., Coyle, B., Ruzov, A., 2017. Immunostaining for DNA modifications: computational analysis of confocal images. JoVE, e56318.
- Richards, E.J., Elgin, S., 2002. Epigenetic codes for heterochromatin formation and
- silencing rounding up the usual suspects. Cell 108, 489–500. Rousseeuw, P.J., 1987. Silhouettes: a graphical aid to the interpretation and validation of cluster analysis. J. Comput. Appl. Math. 20, 53–65.
- Sanchez, O.F., Lee, J., Hing, N.Y.K., Kim, S.-E., Freeman, J.L., Yuan, C., 2017. Lead (Pb) exposure reduces global DNA methylation level by non-competitive inhibition and alteration of dnmt expression. Metall 9, 149-160.
- Sánchez, O.F., Mendonca, A., Min, A., Liu, J., Yuan, C., 2019. Monitoring histone methylation (H3K9me3) changes in live cells. ACS Omega 4, 13250-13259.
- Sánchez, O.F., Lin, L., Bryan, C.J., Xie, J., Freeman, J.L., Yuan, C., 2020. Profiling epigenetic changes in human cell line induced by atrazine exposure. Environ. Pollut. 258, 113712.
- Schneider, J.S., Anderson, D.W., Kidd, S.K., Sobolewski, M., Cory-Slechta, D.A., 2016. Sex-dependent effects of lead and prenatal stress on post-translational histone modifications in frontal cortex and hippocampus in the early postnatal brain. Neurotoxicology 54, 65-71.
- Shefa, S.T., Héroux, P., 2017. Both physiology and epidemiology support zero tolerable blood lead levels. Toxicol. Lett. 280, 232-237.
- Shenoda, B.B., Tian, Y., Alexander, G.M., Aradillas-Lopez, E., Schwartzman, R.J., Ajit, S.K., 2018. miR-34a-mediated regulation of XIST in female cells under inflammation. J. Pain Res. 11, 935.
- Shipley, M.M., Mangold, C.A., of Visualized, S.-M.L., 2016. Differentiation of the SH-SY5Y human neuroblastoma cell line. JoVE 108, e53193.
- Singh, G., Singh, V., Wang, Z.-X., Voisin, G., Lefebvre, F., Navenot, J.M., Evans, B., Verma, M., Anderson, D.W., Schneider, J.S., 2018a. Effects of developmental lead exposure on the hippocampal methylome: influences of sex and timing and level of exposure. Toxicol. Lett. 290, 63-72.
- Singh, G., Singh, V., Wang, Z.-X., Voisin, G., Lefebvre, F., Navenot, J.M., Evans, B., Verma, M., Anderson, D.W., Schneider, J.S., 2018b. Effects of developmental lead exposure on the hippocampal methylome: influences of sex and timing and level of exposure. Toxicol. Lett. 290, 63-72.
- Stefanovski, D., Tang, G., Wawrowsky, K., Boston, R.C., Lambrecht, N., Tajbakhsh, J., 2017. Prostate cancer diagnosis using epigenetic biomarkers, 3D high-content imaging and probabilistic cell-by-cell classifiers. Oncotarget 8, 57278.
- Sun, H., Wang, N., Nie, X., Zhao, L., Li, Q., Cang, Z., Chen, C., Lu, M., Cheng, J., Zhai, H., Xia, F., Ye, L., Lu, Y., 2017. Lead exposure induces weight gain in adult rats, accompanied by DNA hypermethylation. PloS One 12.
- Tan, S.-L., Nishi, M., Ohtsuka, T., Matsui, T., Takemoto, K., Kamio-Miura, A., Aburatani, H., Shinkai, Y., Kageyama, R., 2012. Essential roles of the histone methyltransferase ESET in the epigenetic control of neural progenitor cells during development. Development 139, 3806-3816.
- Teng, J., Takei, Y., Harada, A., Nakata, T., Chen, J., Hirokawa, N., 2001. Synergistic effects of MAP2 and MAP1B knockout in neuronal migration, dendritic outgrowth, and microtubule organization. J. Cell Biol. 155, 65-76.
- Tibshirani, R., 2011. Regression shrinkage and selection via the lasso: a retrospective. J. Roy. Stat. Soc. B 73 (3), 273-282.
- Triantafyllidou, S., L, Y., Edwards, M., 2009. Lead (Pb) exposure through drinking water: lessons to be learned from recent US experience. Global NEST 11 (3), 341.
- Triantafyllidou, S., Nguyen, C.K., Zhang, Y., Edwards, M.A., 2013. Lead (Pb) quantification in potable water samples: implications for regulatory compliance and assessment of human exposure. Environ. Monit. Assess. 185 (2), 1355-1365.
- Tyssowski, K., Kishi, Y., Gotoh, Y., 2014. Chromatin regulators of neural development. Neuroscience 264, 4-16.
- Watanabe, T., Zhang, Z.-W., Qu, J.-B., Gao, W.-P., Jian, Z.-K., Shimbo, S., Nakatsuka, H., Matsuda-Inoguchi, N., Higashikawa, K., Ikeda, M., 2000. Background lead and cadmium exposure of adult women in Xian City and two farming villages in Shaanxi Province, China. Sci. Total Environ. 247, 1–13.
- Weisskopf, M.G., Weuve, J., Nie, H., Saint-Hilaire, M.-H., Sudarsky, L., Simon, D.K., Hersh, B., Schwartz, J., Wright, R.O., Hu, H., 2010. Association of cumulative lead exposure with Parkinson's disease. Environ. Health Perspect. 118, 1609–1613.
- Wilson, N., Horrocks, J., 2008. Lessons from the removal of lead from gasoline for controlling other environmental pollutants: a case study from New Zealand.

- Environ. Health: a global access science source 7, 1.
- Wu, J., Basha, M., Brock, B., Cox, D.P., Cardozo-Pelaez, F., McPherson, C.A., Harry, J., Rice, D.C., Maloney, B., Chen, D., Lahiri, D.K., Zawia, N.H., 2008. Alzheimer's disease (AD)-Like pathology in aged monkeys after infantile exposure to environmental metal lead (Pb): evidence for a developmental origin and environmental link for AD. J. Neurosci. 28, 3–9.
- Xiao, J., Wang, T., Xu, Y., Gu, X., Li, D., Niu, K., Wang, T., Zhao, J., Zhou, R., Wang, H.-L., 2020. Long-term probiotic intervention mitigates memory dysfunction through a novel H3K27me3-based mechanism in lead-exposed rats. Transl. Psychiatry 10, 25.
- Xicoy, H., Wieringa, B., Martens, G.J., 2017. The SH-SY5Y cell line in Parkinson's disease research: a systematic review. Mol. Neurodegener. 12, 10.
- Yan, D., Wang, L., Ma, F.-L., Deng, H., Liu, J., Li, C., Wang, H., Chen, J., Tang, J.-L., Ruan, D.-Y., 2008. Developmental exposure to lead causes inherent changes on

- voltage-gated sodium channels in rat hippocampal CA1 neurons. Neuroscience 153, 436–445.
- Yao, B., Christian, K.M., He, C., Jin, P., Ming, G.-L., Song, H., 2016. Epigenetic mechanisms in neurogenesis. Nat. Rev. Neurosci. 17, 537–549.
- Zenk, F., Loeser, E., Schiavo, R., Kilpert, F., Bogdanović, O., Iovino, N., 2017. Germ line—inherited H3K27me3 restricts enhancer function during maternal-to-zygotic transition. Science 357, 212–216.
- Zhao, Q., Zhang, J., Chen, R., Wang, L., Li, B., Cheng, H., Duan, X., Zhu, H., Wei, W., Li, J., 2016. Dissecting the precise role of H3K9 methylation in crosstalk with DNA maintenance methylation in mammals. Nat. Commun. 7, 1–12.
- Zou, R.-X., Gu, X., Ding, J.-J., Wang, T., Bi, N., Niu, K., Ge, M., Chen, X.-T., Wang, H.-L., 2020. Pb exposure induces an imbalance of excitatory and inhibitory synaptic transmission in cultured rat hippocampal neurons. Toxicol. Vitro 63, 104742.